IMPROVED CARILLON SYNTHESIS

Mark Rau, Orchisama Das, Elliot K. Canfield-Dafilou *

Center for Computer Research in Music and Acoustics,
Stanford University, Stanford, CA 94305 USA
[mrau|orchi|kermit]@ccrma.stanford.edu

ABSTRACT

An improved and expanded method for carillon bell synthesis is proposed. Measurements of a carillon bell and its clapper were made to serve as the basis for an efficient synthesis framework. Mode frequencies, damping, and amplitudes are used to form a modal model fit to measurements. A parameterized clapper interaction model is proposed to drive the bell model, reproducing variation of timbre as the bell is played in different dynamic ranges. Reverberation of the belfry was measured from several listener perspectives and an efficient modal reverberation architecture is shown to model the sound of the bell from locations inside and outside the belfry.

1. INTRODUCTION

Musical acousticians and composers have long held interest in carillons and other bells. Rossing and others seek to understand the physics of how bells vibrate [1, 2]. Others, such as Lehr, work for bell foundries and are interested in improving their casting and tuning techniques [3, 4]. Recently, some researchers have modeled bells using finite element analysis [5]. Romantic composers have often evoked and imitated the sound of bells in their music. Twentieth century works by John Chowning, Jean-Claude Risset, and Jonathan Harvey have all prominently feature synthesized bell timbres. More recent "Hack the Bells" initiatives such as [6] have lead to an increased interest in music for carillon and live electronics.

In contrast to [7], where the authors' goal was to provide a simple model for carillon bell synthesis suitable for processing by composers of electroacoustic music, in this paper we provide a more sophisticated model. Like in previous work, a modal architecture is presented where a bell is modeled as a sum of exponentially decaying sinusoids. One of the issues of [7] was that the authors were limited to a single recording of each bell of the carillon they were modeling. This means they were unable to model the spectral differences between quiet and loud bell hits and were restricted to the perspective of the single microphone.

For this work, we made a comprehensive set of measurements of the bell we model with the idea that the results can be applied for modeling other bells. These measurements include multiple microphone locations, laser Doppler vibrometer (LDV) measurements from the impact position, and accelerometer measurements of the clapper's movement. We additionally made impulse response measurements of the belfry. With these measurements, we perform better when estimating the modal parameters, incorporate a driving function that adequately controls the spectral changes associated with quiet and loud bell strikes, and demonstrate an efficient modal reverberation algorithm allowing the possibility to control and modify the position of the listener.

A carillon is a musical instrument consisting of multiple cup-shaped cast bronze bells. The bells are stationary and struck on the inside by clappers. The bell measured and modeled in this study comes from the Stanford Carillon located in the tower of the Hoover Institution. This carillon consists of thirty-five bells originally cast by Michiels in Tournai, Belgium for the 1939 New York World's Fair [8]. In 2002, The Dutch foundry Royal Eijsbouts recast eleven of these bells and added an additional thirteen bells, bringing the total to forty-eight bells. Additionally, they upgraded several other components of the instrument such as the keyboard and the hanging mechanism. The instrument is equally tempered.

We begin by outlining the measurements of the bell and belfry in §2. Then in §3 we describe the modal synthesis model and how we estimate the various parameters. We discuss results in §4. Finally, §5 offers some concluding remarks.

2. CARILLON BELL MEASUREMENTS

For this study, we measured a large carillon bell tuned to C3, having a fundamental frequency of 129 Hz. An accelerometer was used to measure the keyboard driven clapper interaction while a laser Doppler vibrometer and various microphones were used to measure the resulting bell vibrations. Figure 1 shows the locations of the microphones, LDV, accelerometer, and loudspeaker in relation to the tower, belfry, and bell.

2.1. Clapper Interaction

An accelerometer was placed on the back of the clapper to measure its acceleration as it strikes the bell. It was in line with the clapper's primary direction of motion, orthogonal to the shell of the bell. It was assumed that the arc of the clapper path was negligible and only in one spacial direction. A laser Doppler vibrometer was used to measure the surface velocity at a point on the outside of the bell corresponding to the location of the clapper hit. The measurement locations were chosen to be at an approximation of the driving point, taking physical considerations into account.

2.2. Near Field Radiation

In addition to the contact measurements, several measurement-quality omnidirectional pressure microphones were used to record the sound radiated by the bells at various locations. One microphone was placed in the belfry about 1 m away from the carillon bell to capture the close field radiation. A second microphone was

* All authors should be considered co-first author of this paper.

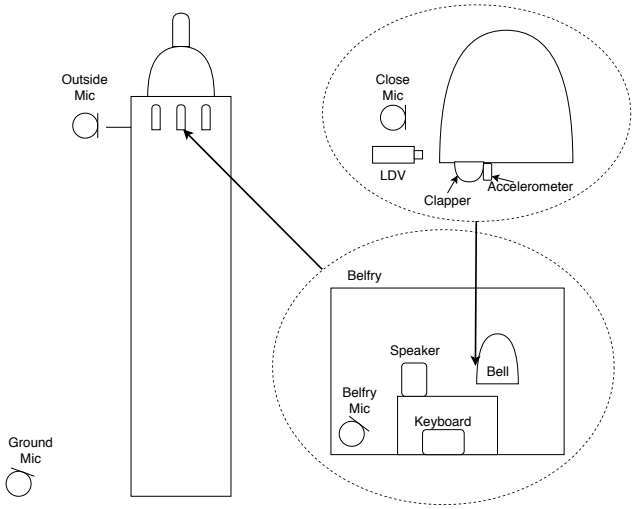

Figure 1: Measurement setup.

placed in the belfry below the bells, in a location similar to where a person may stand in the tower while the carillon is played. A third microphone was suspended on a pole 3 m out of a window in the belfry. This captures the on axis portion of the signal that would pass through the windows of the carillon tower. While this measurement is not from a listener's perspective, it is from an accessible location partway between the belfry and the ground and provides a different prospective of the bell sound.

2.3. Far Field Radiation

In an attempt to measure impulse responses of the bell tower to common listening positions, inexpensive portable recorders were placed at four locations outside of the tower. One recorder was located 25 m from the base of the tower, and the other three were approximately 150, 600, and 1000 m away, at ground level. Two-minute-long exponential sinusoidal sweeps covering the audible frequency range from 20–20000 Hz were played from a loudspeaker in the tower and recorded using all near field and far field microphones. Several of the far field recorders were corrupted by noise caused by other sound sources in the area and the large distance from the tower.

2.4. Bell Coupling

To test if the bells are acoustically coupled, an LDV was used to measure the surface vibration of one bell while other bells were played. Two pairs of bells were tested—one pair was adjacent to each other and the other tonally separated by an octave. In both cases, no significant coupling was measured, so this was not considered further in the model.

3. MODAL CARILLON BELL MODEL

The sound of a bell can be described as an inharmonic series of partials. Like in [7], we use a modal model to represent each bell as a sum of exponentially decaying sinusoids,

$$g(t) = \sum_{m=1}^{M} \alpha_m e^{j\omega_m t} e^{-t/\tau_m}, \qquad (1)$$

where α_m is the complex amplitude, ω_m the frequency, and τ_m the decay rate for each mode m.

Throughout this section, we will describe our methods for estimating the modal parameters for synthesizing carillon bell sounds. We extend the modal analysis proposed in [7] using simple and robust methods rather than complex high resolution methods such as the one described in [9].

3.1. Estimating Partial Frequencies

First, the clapper impact is deconvolved from the time domain bell measurements. Then, all ten measurements at different loudness levels are averaged in the time domain for further analysis. This improves the signal to noise ration (SNR) as the spectral peaks are common in all measurements. Additionally, nulls in the spectrum of the clapper are dependent on the loudness of the strike while the mode parameters of the bell itself should be independent of loudness. By averaging recordings at several loudness levels, we reduce the bias in the peak picking and amplitude fitting that would over-fit to a single bell loudness.

Similar to [7], the deconvolved bell signal is high-passed filtered half an octave below the hum tone before its Fourier Transform is taken. This reduces the likelihood of picking spurious peaks in the lower frequencies that are simply background noise.

The method for peak picking proposed in [7] is not able to detect close-frequency beating partials (doublets) and it misses a number of high frequency partials which decay very quickly, resulting in inaccurate reconstruction of the bell attack. The following subsections explain the updated method for overcoming these shortcomings.

3.1.1. Resolving doublets

In the previous method, peaks that were very close to each other were discarded. For resolving doublets, this constraint is removed. Even with a larger FFT size, resolving doublets can be tricky. The Hann window used in [7] has a side lobe height of -31.5 dB. This poses the danger of partial side lobes being detected as peaks. To fix this, we use the Hann-Poisson window (2) instead, which is essentially a Hann window multiplied with an exponentially decaying Poisson window [10]. The advantage of this window is that for $\gamma \geq 2$, the side-lobes are smoothed. For high γ, this window has no side-lobes. With the Hann-Poisson window, the peaks detected are guaranteed to be partials and not their side-lobes.

$$w(n) = \frac{1}{2}\left[1 + \cos\left(\frac{2\pi n}{M-1}\right)\right] \exp\left(\frac{-2\gamma|n|}{M-1}\right) \qquad (2)$$

3.1.2. Adaptive threshold for peak picking

In the previous method, the threshold for peak picking was kept constant. However, as can be seen from Fig. 2, the spectral envelope shape is not flat, but resembles a low-pass filter. This means that a constant threshold will not be able to detect higher partials, which fall below it. A smarter decision is to pick a threshold that follows the spectral envelope. To do so, first we use a median filter with a filter order of 100 to smooth the spectrum and estimate the spectral envelope. We then fit a straight line to the spectral envelope, and add a constant value to it to get the new threshold. Flattening the spectrum with a "pre-emphasis" filter would have also worked.

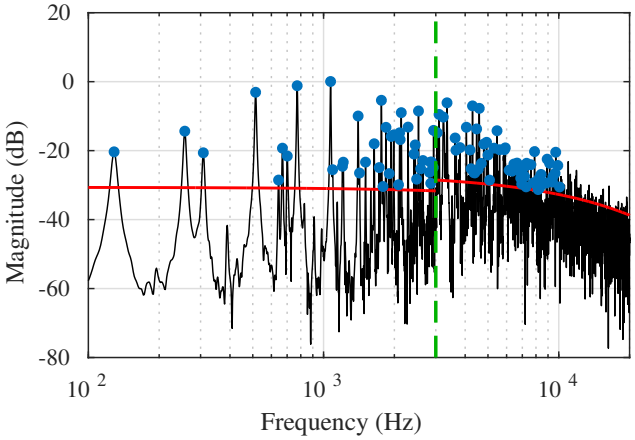

Figure 2: Mode frequency estimates.

3.1.3. Two FFT sizes

We pick two different FFT sizes for low and high frequency partials, with a transition frequency at 3 kHz. A larger FFT size of 2^{15} for detecting lower partials ensures that beating partials are resolved. For higher frequency partials, resolution is not an issue. Lower partials have a small beat frequency, however the beat frequency increases for higher partials, which is why resolving high frequency doublets is possible with a smaller FFT size. Instead, too large an FFT size for higher partials results in poor signal to noise ratio in estimation of decay rates. So, we choose an FFT size of 2^{13} for higher partials. For lower partials, we use a Hann-Possion window with $\gamma_l = 7$ and for higher partials, $\gamma_h = 3$. We can get away with less smoothing of side lobes for higher partials because we ensure that two nearby candidate peaks are not detected as two separate partials. This ensures no side lobes are incorrectly labeled as partial peaks. The peaks picked with two different FFT sizes are shown in Fig. 2. We do not detect any peaks above 10 kHz because the accelerometer is band-limited and there is a high noise floor so we are not confident in the measurements in this region. Instead, we statistically generate higher frequency modes as described in §3.4.

3.2. Estimating Partial Decay Rates

As in [7], we use each frequency found in §3.1 as the center frequency for a fourth-order Butterworth band-pass filter. We find the energy envelope for each partial by averaging the band-pass filtered signals using a 100 ms RMS procedure. However, in [7], the decay rate of each partial was estimated by performing a linear fit to the amplitude envelope using least squares. The region over which the linear fit was performed was selected manually. Since many more partials are detected in our updated method, this procedure is inefficient and time consuming. Instead, we use the method in [11] to automatically estimate the decay rates. This algorithm is based on nonlinear optimization of a model for exponential decay plus stationary noise floor. It works well, even for beating partials that are coupled. For higher modes that decay quickly, we use a weighting function that fits an exponential decay only over the first second of the energy envelope and discards the rest, so that high frequency noise does not perturb the calculation of decay rates. This method was rejected in [7] because the SNR of the single-bell recordings often challenged the algorithm. Here, our SNR is much higher so the algorithm performs better. A disadvantage of this method is that it solves a large optimization problem, and is therefore, quite slow.

3.3. Estimating Partial Amplitudes

Once we have estimated the frequency and decay rate of each mode, we estimate the initial amplitude of each partial required to reconstruct the original bell recording. To do this, we form a matrix where each column holds each partial independently as in

$$\mathbf{M} = \begin{bmatrix} 1 & \dots & 1 \\ e^{(j\omega_1 - 1/\tau_1)} & \dots & e^{(j\omega_M - 1/\tau_M)} \\ \vdots & \dots & \vdots \\ e^{(j\omega_1 - 1/\tau_1)T} & \dots & e^{(j\omega_M - 1/\tau_M)T} \end{bmatrix}, \tag{3}$$

where $\boldsymbol{\omega}_m$ are the frequencies, $\boldsymbol{\tau}_m$ the decay rates, and T is the length of the time vector. We use least squares to find the complex amplitudes

$$\boldsymbol{\alpha} = (\mathbf{M}^\intercal \mathbf{M})^{-1} \mathbf{M}^\intercal \boldsymbol{g}\,, \tag{4}$$

where $\boldsymbol{g}$ is the original bell recording and $\boldsymbol{\alpha}$ is the vector of complex amplitudes.

3.4. Statistically Generating High Frequency Modes

While the low frequency modes are louder and decay more slowly than the high frequency modes, the high modes play a role in developing the transient attack sound. It is difficult to measure and estimate modal parameters for the high modes for a variety of reasons. The signal energy at high frequencies is much lower than the low frequencies and the noise floor becomes a significant impediment. Additionally, the measurements from the accelerometer are band-limited, making it impossible to accurately estimate the high frequency modes.

Since the resonant structure of the bell is inharmonic and human hearing has low acuity in high frequencies, it is possible to synthesize artificial high frequency modes. The idea here is to synthesize enough high frequency modes to produce the transient sound without increasing the computational cost too much. To do this, we generate a set of modal frequencies above the frequency we stop fitting modal parameters, i.e. 10 kHz. Figure 3a shows the frequency of estimated modes in black circles, along with the cut-off frequencies of the Bark critical bands of hearing in grey [12]. We can see that mode density increases with critical band number. We fit a quadratic function along with some sinusoidal modulation to the existing mode frequencies and generate new mode frequencies in the range of 10–16 kHz (shown as blue crosses). For the decay rates and amplitudes, we extrapolate from the lower modes. We fit a decaying exponential to the existing decay rates to generate new data points (Fig. 3b). For the amplitudes, we sample from a Gaussian distribution with a mean given by that of the estimated mode amplitudes from §3.3 and a variance of 10^{-5} (Fig. 3c).

3.5. Modeling the Bell-Clapper Interaction

Previous literature suggests that when the carillon is performed at higher dynamic ranges, the high harmonics become more prominent in the timbre. It is suggested that this change in timbre is due to the contact time of the clapper interaction, with a louder hit

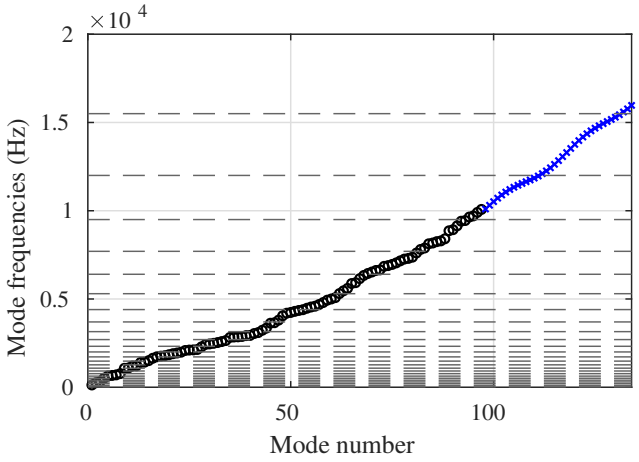

(a) Extrapolated mode frequencies (Bark band cutoff frequencies in grey).

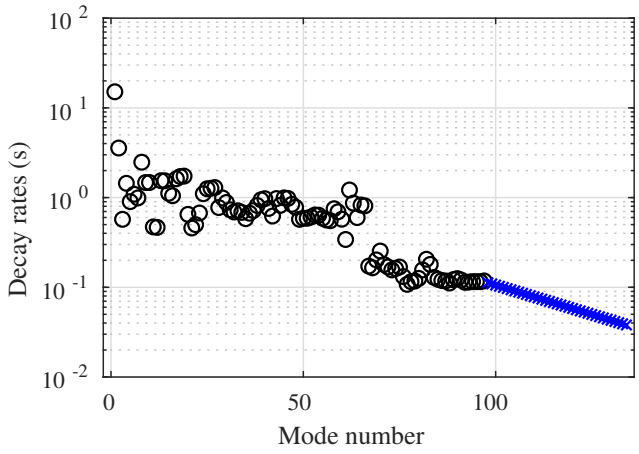

(b) Extrapolated mode decay rates.

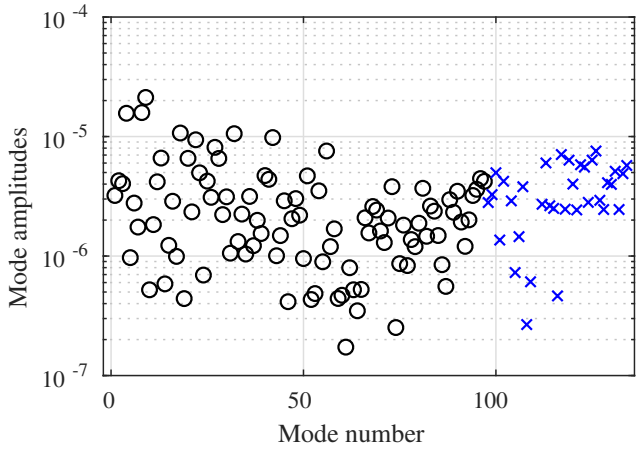

(c) Extrapolated mode amplitudes.

Figure 3: Extrapolated mode parameters (in blue crosses).

having a shorter contact time [13, 14]. To confirm this effect, the clapper acceleration of the initial impact was recorded during nine different dynamic levels. It was assumed that the acceleration of

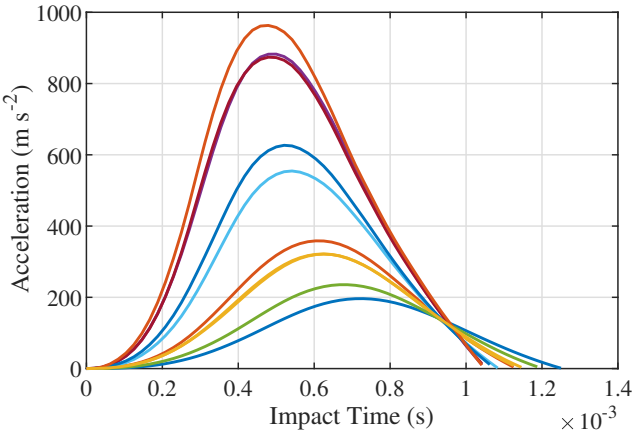

(a) Time domain.

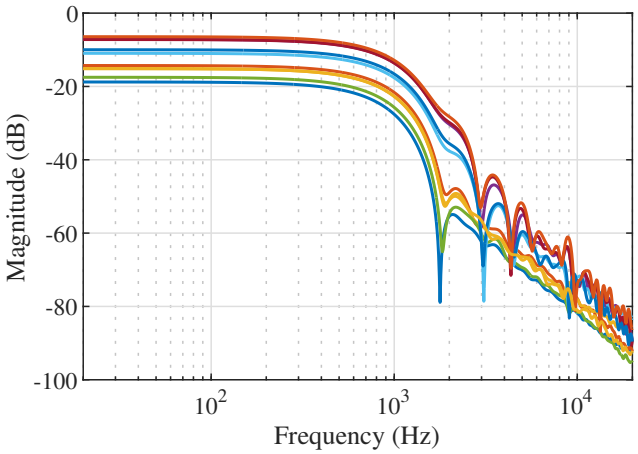

(b) Frequency domain.

Figure 4: Measured impact acceleration of the clapper striking the bell.

the clapper during the time when it was in contact with the bell is proportional to the force exerted by the clapper, so the acceleration can be used as an input signal to drive the carillon model. The measured acceleration during impact of nine hits as well as the corresponding frequency response of the impulses are shown in Fig. 4.

As confirmed by our measurements, when the carillon is performed at a louder dynamic level, the impact time is shorter and the pulse shape changes in an asymmetrical manner. The frequency response shows that the locations of the nulls change, and the louder hits boost frequencies in the range of 1.5–3 kHz in relation to the quiet hits.

To create a musically usable synthesis model, it is desirable to have as few variable parameters as possible. In this case, it would be ideal to have one parameter for strike amplitude which can drive the carillon model. There have been multiple solutions proposed to model the impact ranging from a half-cycle sine wave proposed by Rayleigh [15], or a Gaussian [5], to numerical solutions [5, 16, 17]. However, the half-cycle sine wave and Gaussian solutions are oversimplified and a numerical solution is not practical for real-time synthesis, so a compromise was made to generate

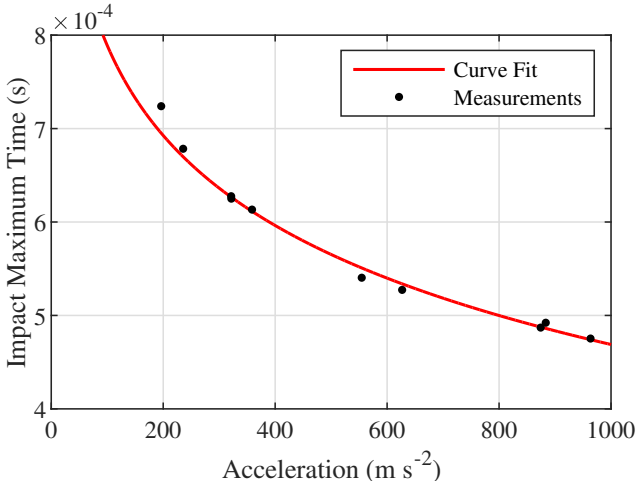

(a) Impact peak time as a function of impact acceleration.

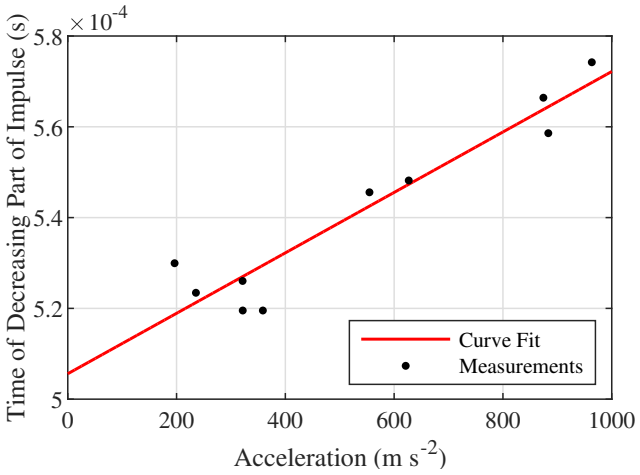

(b) Time of the decreasing portion of the impact as a function of impact acceleration.

Figure 5: Data used to fit curves for parameterized clapper impact model.

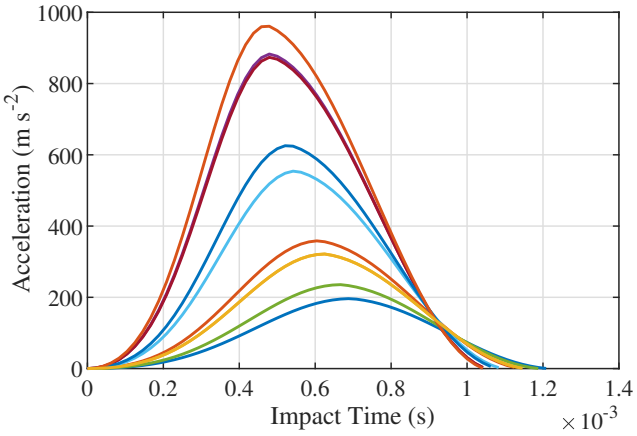

(a) Time domain.

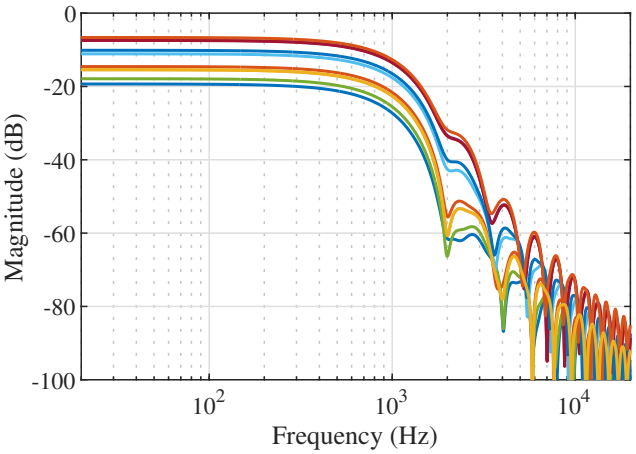

(b) Frequency domain.

Figure 6: Synthesized impact acceleration of the clapper striking the bell.

impact signals which are created to fit the data and are parameterized by the impact peak acceleration.

The two defining characteristics of the impacts were chosen to be the time of the acceleration peak and the length of the decreasing portion of the acceleration. Figure 5a shows the time of the acceleration peak plotted against the peak acceleration, while Fig. 5b shows the time taken for the acceleration to decrease to zero after the peak acceleration, against the peak acceleration.

The impact peak time was fit using the logarithmic function:

$$p(a_p) = \frac{-\ln\left(\frac{a_p}{29170(ms^{-2})}\right)}{7193(s^{-1})}, \quad (5)$$

where a_p is the peak amplitude, and ln is the natural logarithm. The time taken for the impact acceleration to decrease was fit using the linear function:

$$d(a_p) = 6.658 \times 10^{-8}(m^{-1}s^3) \times a_p + 5.056 \times 10^{-4}(s), \quad (6)$$

where a_p is the peak amplitude. The curve fits are shown in Fig. 5a and 5b.

Synthesized clapper impulses were created by combing the left and right portions of two window functions. The left portion of the impulse is the left half of a Blackman window,

$$w_l(n) = 0.42 - 0.5\cos\left(\frac{2\pi n}{N}\right) + 0.08\cos\left(\frac{4\pi n}{N}\right), \quad (7)$$

for $0 \leq n \leq N-1$, where $N = 2f_s \times p(a_p)$, and f_s is the sample rate. The right portion of the impulse is the right half of a Bartlett-Hann window,

$$w_r(m) = 0.62 - 0.48\left|\frac{m}{M} - 0.5\right| - 0.38\cos\left(\frac{2\pi m}{M}\right), \quad (8)$$

for $0 \leq m \leq M-1$, where $M = 2f_s \times d(a_p)$ [10]. These windows are parameterized by the peak amplitude of the desired hit (a_p), and created to be of length $2p(a_p)$ and $2d(a_p)$ seconds respectively for the Blackman an Bartlett-Hann windows. Figure 5 shows time and frequency domain plots of synthesized impact signals having the same peak acceleration as the measured impacts shown in Fig. 4.

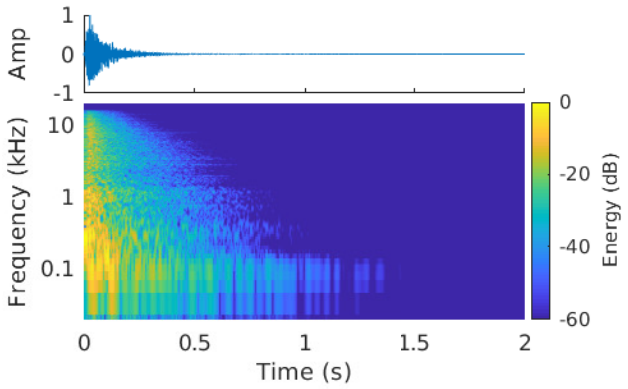

(a) Belfry impulse response.

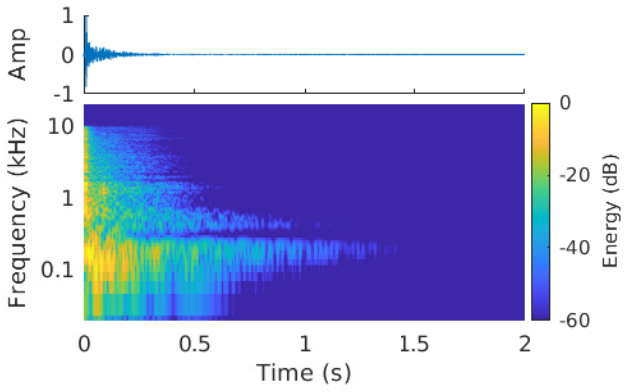

(b) Ground impulse response.

Figure 7: Impulse responses taken from Hoover tower.

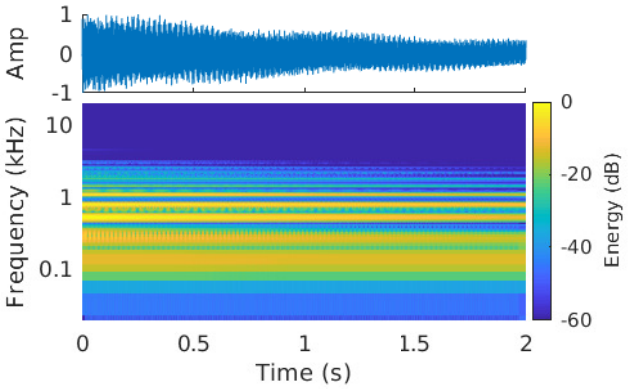

(a) Synthesized bell.

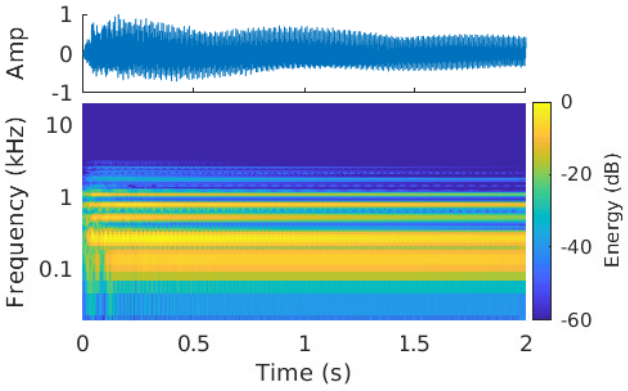

(b) Synthesized bell with belfry convolution reverb.

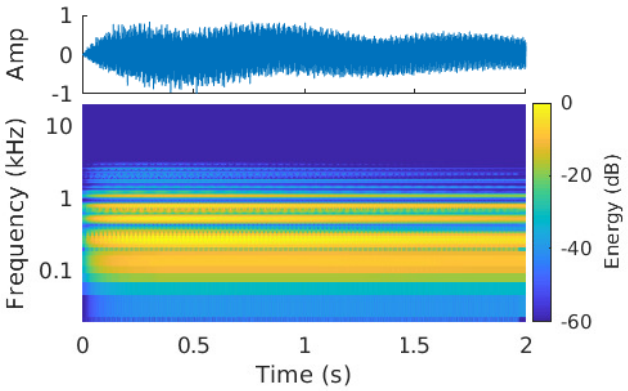

(c) Synthesized bell with efficient modal reverb.

Figure 8: Comparison of a synthesized bell without reverb (8a), with convolution reverb (8b), and with an efficient modified modal reverb (8c).

3.6. Efficient Belfry Reverberation

The belfry where the bells are housed can have a large impact on the sound of a carillon in addition to affecting how the sound radiates from the tower. Figure 7 shows impulse responses of the reverberation of Hoover tower measured 3 m outside the belfry and from the bottom of the tower. The response from the bottom of the tower contains much less high-frequency energy and has a prominent slapback echo from a nearby building. Needless to say, the bells sound very different from inside the tower.

The sound of a carillon bell ringing in a belfry can be represented as the convolution of the bell with the reverberation of the belfry. Since we are using a modal bell model, we can also implement the reverberation with a modal architecture [18]. The computation time is independent of the fact that this architecture is a combination of series and parallel components. For each time step, the number of operations scales linearly with the total number of modes. That being said, we can implement an even more efficient reverberation algorithm by taking advantage of the modal architecture.

Most of the modes of the carillon bell are orthogonal to most of the modes of the reverb. If we assume that the majority of the energy of each bell mode only drives the reverb modes that are close in frequency, we find an efficient way to implement the reverbera-

tion. Instead of processing each mode of the bell through the full complement of reverberation modes, we can pass each bell mode through the reverberation mode nearest in frequency. Furthermore, we fold the reverberation model into the bell model by replacing the decaying exponential amplitude envelopes of the bell modes and reverberation modes by the convolution of the envelopes. Now (1) can be replaced by

$$g(t) = \sum_{m=1}^{M} \alpha_m \beta_m e^{j\omega_m t} \frac{\tau_m \zeta_m \left(e^{-t/\tau_m} - e^{-t/\zeta_m} \right)}{\tau_m - \zeta_m}, \quad (9)$$

where β_m is the amplitude and ζ_m the decay rate of the belfry reverberation nearest the m^{th} mode where the frequency term is shared for the bell and reverb. Figure 8 shows a synthesized bell without reverb and the same bell resynthesized with the belfry reverberation implemented with convolution reverberation and with the efficient scheme shown in (9).

4. RESULTS AND DISCUSSION

Sound examples of the original measurements and resynthesized bells with and without reverb can be found at `https://ccrma.stanford.edu/~kermit/website/morebells.html`. The modal bell driven with synthesized impacts to emulate different loudness levels is shown in Fig. 9. As the impact force on the bell increases, higher modes become more perceptually prominent and ring longer. There is also more energy imparted into all modes, as is intuitive and clear from the figure. A comparison of a measured and modeled bell strike can be seen in Fig. 10. Note that the resynthesized bell has significantly less noise than the recording but they otherwise sound similar.

The clapper interaction model is simple and controlled by one parameter, providing a reasonable approximation of the spectral variation one would expect when playing a carillon at varying dynamic ranges. However, the model is an approximation based on measurements and not derived analytically from the physics governing contact dynamics of the interaction. This leads to the high frequency nulls not appearing at the exact location of the measured impulses. A more accurate model based on the physics would be a large improvement, but it must be easily parameterizable and require low computation to be useful in a performance context.

The efficient reverberation algorithm presented in §3.6 does not sound exactly the same as the convolution reverb. This is due to the fact that some energy spreads to modes at other frequencies. One solution to this issue would be to compute a small subset of the reverberation modes for each bell mode. At the expense of a little more computation, this will more accurately implement the reverberation. Another possibility would be to implement a hybrid reverberation algorithm where the efficient modal implementation is used in combination with a short FIR filter containing the a windowed version of the few milliseconds of the belfry reverberation with the shared mode frequencies removed. This would implement the mode coupling while remaining computationally efficient.

5. CONCLUSION AND FUTURE WORK

In this paper, we have proposed an accurate modal model of a carillon bell capable of being driven by different impact functions which have been derived from physical measurements of the clapper striking the bell. Artificial high frequency modes have been

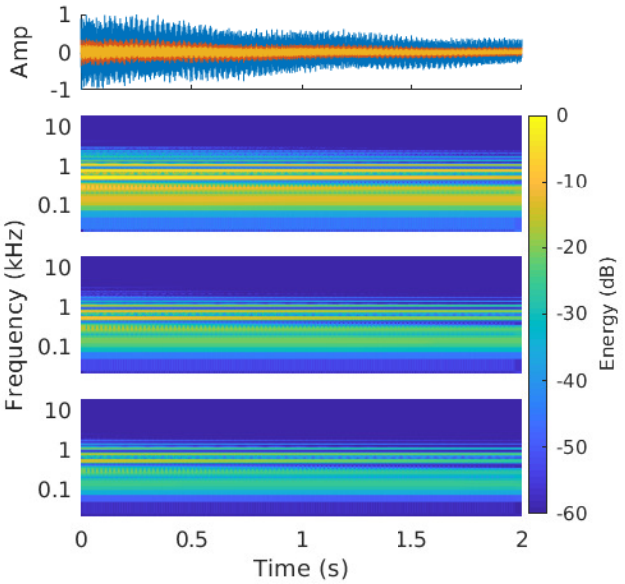

Figure 9: Synthesized bell at different dynamic levels: ***ff*** (top), ***mf*** (middle), and ***p*** (bottom).

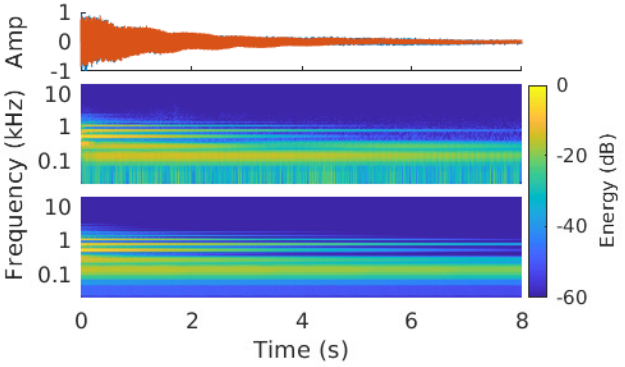

Figure 10: Measured bell (top) and modeled bell (bottom).

generated using data extrapolation for more accurate reconstruction of the bell transient. We also measured the belfry impulse responses and proposed an efficient implementation of the belfry reverberation with a modal architecture. This model is more accurate than previous attempts, can be run real-time, and takes musical dynamics into consideration. We hope that this added flexibility in modeling bells will aid composers to conceive pieces with novel and interesting uses of the carillon bell aided with live electronics.

A method for modeling bells has been presented, but has only been tested on one bell. Future work may include further validation on multiple bells. Of particular interest is testing how the clapper interaction model will translate to smaller bells. We attempted to measure a smaller bell as well, but the accelerometer clipped due the higher acceleration of the less massive clapper. We hope

to continue working on carillon models to increase their accuracy and expand the flexibility for composers.

6. ACKNOWLEDGMENTS

The authors thank Stanford University Carillonneur Timothy Zerlang and the Hoover Institution for providing access to the carillon and Hoover Tower.

7. REFERENCES

[1] Thomas Rossing and Robert Perrin, "Vibrations of bells," *Applied Acoustics*, vol. 20, pp. 41–70, 1987.

[2] Thomas Rossing, Ed., *The Acoustics of Bells*, Van Nostrand Reinhold, 1984.

[3] Andre Lehr, "Designing chimes and carillons in history," *Acta Acustica united with Acustica*, vol. 83, no. 2, pp. 320–36, 1997.

[4] Andre Lehr, "The removal of warbles or beats in the sound of a bell," *Acta Acustica united with Acustica*, vol. 86, no. 3, pp. 550–6, 2000.

[5] Bjrn-Andre Lau, Peter Wriggers, Albrecht Schneider, and Rolf Bader, "Finite-element transient calculation of a bell struck by a clapper," in *Concepts, Experiments, and Fieldwork: Studies in Systematic Musicology and Ethnomusicology*, pp. 137–56. Peter Lang, 2010.

[6] "University of Michigan hack the bells," https://gobluebells.wordpress.com/2016/09/21/hackthebells/, 2016.

[7] Elliot Kermit Canfield-Dafilou and Kurt James Werner, "Modal audio effects: A carillon case study," in *Proceedings of the International Conference on Digital Audio Effects*, 2017.

[8] Elena S. Danielson, *For peace alone do I ring: The history of the Hoover Tower carillon and its restoration*, Hoover Institution, 2002.

[9] Corey Kereliuk, Woody Herman, Russel Wedelich, and Daniel J. Gillespie, "Modal analysis of room impulse responses using subband esprit," in *Proceedings of the International Conference on Digital Audio Effects*, 2018.

[10] Julius O. Smith, *Spectral Audio Signal Processing*, W3K publishing, 2011.

[11] Poju Antsalo, Aki Makivirta, Vesa Valimaki, Timo Peltonen, and Matti Karjalainen, "Estimation of modal decay parameters from noisy response measurements," in *Proceedings of the 110th Audio Engineering Society Convention*, 2001.

[12] Eberhard Zwicker, "Subdivision of the audible frequency range into critical bands (frequenzgruppen)," *The Journal of the Acoustical Society of America*, vol. 33, no. 2, pp. 248, 1961.

[13] Neville H. Fletcher, William T. McGee, and Alex Z. Tarnopolsky, "Bell clapper impact dynamics and the voicing of a carillon," *The Journal of the Acoustical Society of America*, vol. 111, no. 3, pp. 1437–44, 2002.

[14] Jim Woodhouse, James C. Rene, Catherine S. Hall, Luke T. W. Smith, Frank H. King, and John W. McClenahan, "The dynamics of a ringing church bell," *Advances in Acoustics and Vibration*, vol. 2012, 2012.

[15] John William Strutt and Baron Rayleigh, *The theory of sound*, Dover, 1945.

[16] Piotr Brzeski, Tomasz Kapitaniak, and Przemysław Perlikowski, "Experimental verification of a hybrid dynamical model of the church bell," *International Journal of Impact Engineering*, vol. 80, pp. 177–84, 2015.

[17] Jernej Klemenc, Andreas Rupp, and Matija Fajdiga, "Dynamics of a clapper-to-bell impact," *International Journal of Impact Engineering*, vol. 44, pp. 29–39, 2012.

[18] Jonathan S. Abel, Sean Coffin, and Kyle Spratt, "A modal architecture for artificial reverberation with application to room acoustics modeling," in *Proceedings of the 137th Convention of the Audio Engineering Society*, 2014.